

CONTROL OF TRACTION DRIVE WITH PMSM FROM VIEWPOINT OF EMI

Radovan Doleček¹, Ondřej Černý²

The paper deals with the EMI problems of the individual traction drive of tram wheel. The drive utilizes permanent magnet synchronous motor (PMSM). Until now the major attention has been paid to the control methods of this drive. Nowadays when these control methods are mastered the consideration is focused particularly on interference of designed converter of this drive to near-field environment in which are located other devices. The particular working modes of drive and their interference are demonstrated in this paper. Findings will lead to next steps for reducing of this interference which can bring about fault state of device.

Key words: drive, motor, interference, measurement, near-field, EMI

1 Introduction

The present trend in modern traction drives leads to the utilization of synchronous motors for individual drive. For example a few prototypes of vehicles with permanent magnet synchronous motors (PMSMs) were built and tested in [1], [2], [3], [4], [5] and two prototypes of rail vehicles were presented on InnoTrans fair in Berlin 2008 – Alstom AGV high speed train and Škoda Transportation low floor tram 15T “ForCity”.

PMSMs have better mechanical and electrical advantages in comparison with other types of drive. The torque from viewpoint of dimension and weigh of drive is the greatest advantage. This characteristic makes possible realization so-called direct drive (i.e. drive of axle or wheels without use of any gearbox) from viewpoint of vehicle construction. Direct drives with other motors (e.g. asynchronous motors - ASMs) are not possible to place in vehicle because they have too big dimensions. Applications of simple direct drive of wheel simplify the whole construction of low-floor vehicle from mechanical viewpoint. This simplification of construction leads to time and financial savings from viewpoint of maintenance and other operating costs.

¹ Ph.D. Radovan Doleček, University of Pardubice, Jan Perner Transport Faculty, Department of electrical and electronical engineering and signalling in transport, Studentská 95, 532 10 Pardubice, Czech Republic, tel.: +420 466 036 427, E-mail: radovan.dolecek@upce.cz

² M.Sc. Ondřej Černý, University of Pardubice, Jan Perner Transport Faculty, Department of electrical and electronical engineering and signalling in transport, Studentská 95, 532 10 Pardubice, Czech Republic, tel.: +420 466 036 387, E-mail: ondrej.cerny@upce.cz

2 Research workplace

The research workplace consists of the testing stand which was lent from Research institution rail vehicles to laboratories of Jan Perner Transport Faculty. The current testing stand contains a drive wheel unit (e.g. conception of direct drive without gearbox). The simplest structure of drive creates conditions for good drive characteristics of vehicle, see Fig.1.

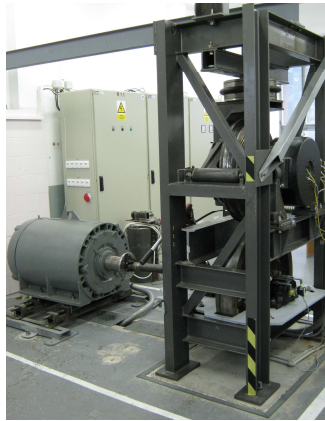


Fig.1: Testing stand.

PMSM prototype type SRT 225-S44 by VÚES Brno has 44 poles, inner rotor and liquid cooling, see Fig.2. It is placed in silent blocks which enable its swing in horizontal direction. Wheel is situated on swinging arm pushed by pneumatic roller. This roller makes pressure to wheel up 4 to 50 kN which represents pressure of real wheel from vehicle.

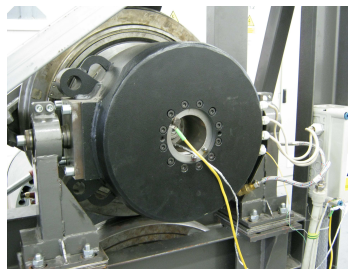


Fig. 2: Synchronous motor with permanent magnets.

The motor type MAF315S-10 by MEZ Brno-Drásov is used as loading drive for tests. This ASM is connected with axle of endless rail of stand by clutch. The torque sensor with dimension ± 1000 Nm is between clutch and endless rail. This loading drive is fed from converter MICROMASTER 440 by Siemens. The converter is completed by breaking converter which enables breaking of whole drive. The speed sensor, which gives possibility of speed feedback for frequency converter of loading drive, is placed on asynchronous drive. The loading drive operates in recuperative mode made by feeding from the same DC intermediate circuit for both converters. Energy losses on breaking resistor are supposed only for emergency out of machine, see Fig.3.

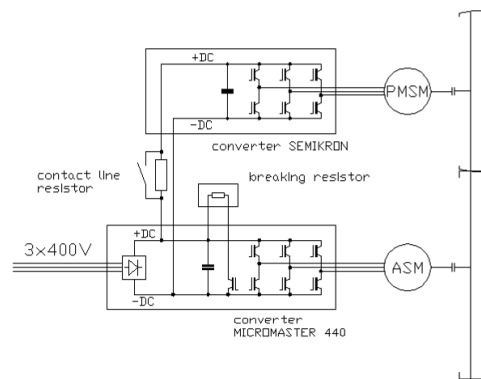


Fig. 3: Diagram of converters structure.

Originally developing converters for PMSM were designed and realized at Jan Perner Transport Faculty, University of Pardubice. The converter power part type B6CI 1100-772-175F by SEMIKRON enables tests under full-load. The converter consists of three double transistors IGBT units SKM400GB124D and has three exciters type SKHI22A. These exciters are constructed only in elementary connection, thus it was necessary to do adjustment of input control and output fault voltage signals. Input circuit of converter is represented by capacitors with total capacity $4700 \mu\text{F} / 1200 \text{V}$. This converter was built up in switchboard for reason of safety and electromagnetic interference. Control system with processor TMS320C2812 by Texas Instruments is placed on board by ŠKODA Electric. More information can be found in [6], [7], [8].

3 Research work

Firstly, the major attention has been paid to control methods of this drive [9], [10], [11]. Nowadays the consideration is focused on interference of this drive to near-field environment, in which are located other devices, and also to supply network. The main current attention is concentrated on EMC problems [12].

3.1 EMI measurement

The circuit boards, antennas and other conductive components all radiate or reflective RF energy. The RF energy from a radiating or reflective object can be coupled into a field probing antenna by inductive, coupling, capacitive coupling or by free-space propagation [13], [14], [15]. The first two coupling methods, also known as reactive or evanescent coupling, exist only for a distance of a few wavelengths from the object surface. Conversely, free-space propagation exists over very large distances. There are three area of propagation relative to a radiating or reflective object [16]:

- The area nearest the radiating object is the reactive or evanescent near-field area. This area includes both propagating and reactive energy. The evanescent energy component decays very rapidly with distance and has completely decayed at a distance of several wavelengths away from the object surface. Properties: Separate E-field and H-field measurements are required to determine the power density and field impedance, the power density decays very rapidly with distance, this area is where near-field circuit board and cable EMI emission measurements are generally made.
- The second area is the radiating near-field or Fresnel area which starts approximately one wavelength away from the radiating object. This area consists of propagating energy with a relatively constant power density. Properties: E-field and H-field measurements are directly interrelated by the impedance of free space (377Ω), the power density remains relatively

constant with distance, this area is where near-field antenna measurements and chamber imaging measurements are typically made.

- The area furthest from the radiating object is the Fraunhofer or far-field area. The transition distance R for the far-field area is generally a distance where the phase curvature of the phase front is 22.5 degrees or

$$R = \frac{2 D^2}{\lambda} \tag{1}$$

where D is largest dimension of radiating object, λ is wavelength. Properties: E-field and H-field measurements are directly interrelated by the impedance of free space (377Ω), the power density decays according to the inverse square law, this is the area for far-field testing.

While approximate distance limits between regions are shown, the actual transition between the regions is quite gradual. Phase coherent measurements of a phasefront in either a propagating near-field or far-field area can be converted into an angle domain far-field equivalent by a Fourier transform based algorithm.

To find source of the emission at circuit level of the object, near-field probes were used. A typical EMI antenna is physically too large to make these measurements. The HZ530 probes set can be used to locate and qualify EMI sources, as well as evaluate EMI problems at the breadboard and prototype level. They enable the user to evaluate radiated fields and perform shield effectiveness comparisons. Mechanical screening performance and immunity tests on cables and components are easily performed. The probes with a built-in pre-amplifier covering the frequency range from 100 kHz to 1 GHz. One main object for interference was converter SEMICRON with IGBT elements. The measuring of converter control signals and their spectra is shown on Fig. 4 and Fig. 5. The measuring was done for levels, see Tab. 1.

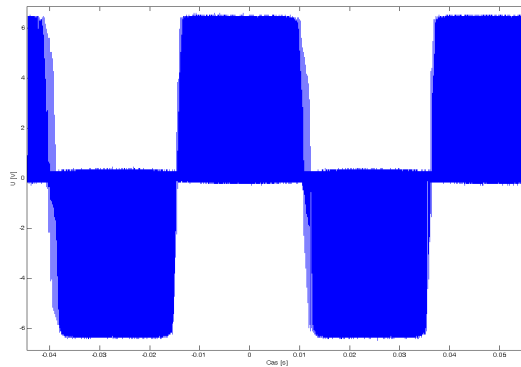


Fig. 4: Converter control signals.

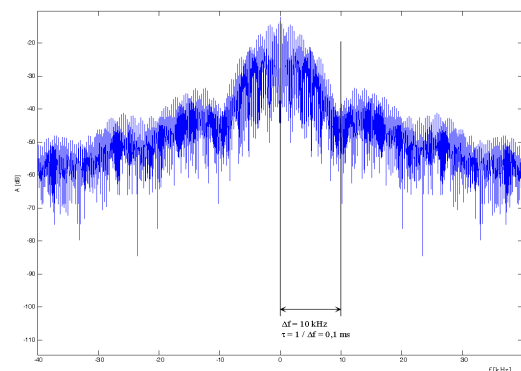


Fig. 5: Spectra of control signals.

Tab. 1: Parameters and their values for measurements, where I_{ef} is effective current of motor and U_{DC} is DC circuit voltage of converter.

Parameter	Value
I_{ef1}	6.12 A (4.2%)
U_{DC1}	559 V
I_{ef2}	97.6 A (80%)
U_{DC2}	498 V
I_{ef3}	122 A (100%)
U_{DC3}	477 V

Firstly, it was necessary to confirm that measuring in frequency range up to 1 GHz is not suitable, because radiating energy at high frequencies is negligible, see Fig.6.

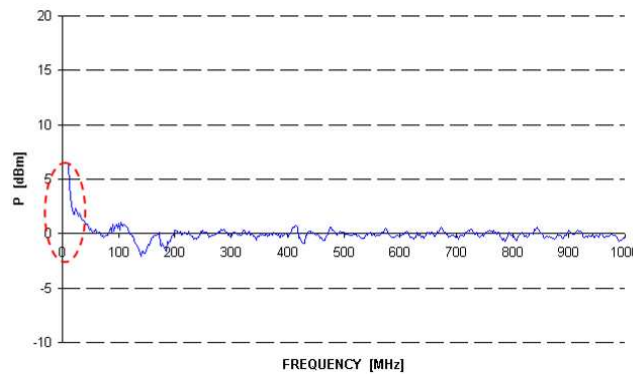


Fig.6: Values of electromagnetic energy.

From this reason, the area with frequency range from 100 kHz - 10 MHz was chosen. The results of measuring for three levels are demonstrated on Fig.7. The red color represents measuring No.1, green color represents measuring No.2, violet color represents measuring No.3 and black color is curve of radiating background when the testing stand and also converters are switched off.

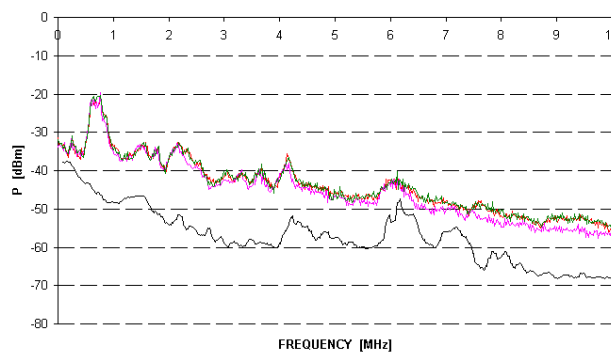


Fig. 7: Values of electromagnetic energy.

4 Conclusion

The results from the measuring confirm that increase of motor current (i.e. motor power) leads to increase of radiating energy from converter. The other EMI measuring according to different methods will continue in order that it would be possible to describe behavior of the whole traction drive very carefully at all operating modes. The specification of radiating energy can bring better shielding solution of this drive and can prevent the interference from radiating.

Acknowledgments

The work on this project was supported by the Czech Grant Agency under grant No. 102/09/P253.

Reference literature

1. J. Novák: “Usage of the synchronous motors at transport means - Part 1”, Journal ELEKTRO, vol.2006, no.6, pp. 4-7, Prague.
2. J. Novák: “Usage of the synchronous motors at transport means - Part 2”, Journal ELEKTRO, vol.2006, no.7, pp. 8-11, Prague.
3. J. Novák: “Usage of the synchronous motors at transport means - Part 3”, Journal ELEKTRO, vol.2006, no.8, pp. 76-78, Prague.
4. K. Yoshida: “Development of main circuit system using direct drive motor (DDM)”, JR East Technical Review Japan, no. 1, pp. 46-52, 2002.
5. M. Osawa: “Toward creation of a railway car meeting the 21st-century requirements”, JR East Technical Review Japan, no. 1, pp. 9-12. 2002.
6. J. Novák: “Means for microprocessing control of electrical drives - Part 1”, Journal ELEKTRO, vol. 2007, no.17, pp. 4-6, Prague.
7. J. Novák: “Means for microprocessing control of electrical drives - Part 2”, Journal ELEKTRO, vol. 2007, no.7, pp. 4-6, Prague.
8. J. Novák: “Means for microprocessing control of electrical drives - Part 3”, Journal ELEKTRO, vol. 2007, no.8, pp. 78-82, Prague.
9. J. Šimánek, J. Novák, O. Černý, and R. Doleček: “FOC and flux weakening for traction drive with permanent magnet synchronous motor”, IEEE International Symp. on Industrial Electronics, pp. 753 – 758, United Kingdom 2008.
10. J. Šimánek, R. Doleček and O. Černý: ”PMSM Drive Control Based on Sinusoidal Commutation Control of Brushless DC Motor”, International Carpathian Control Conf., pp. 615-618, Romania, 2008, ISBN 978-973-746-897-0.
11. J. Šimánek, J. Novák, R. Doleček and O. Černý: “Control algorithms for permanent magnet synchronous traction motor”, Proceedings no. 257, Poland, 2007, ISBN 1-4244-0813-X.
12. J. Novák, J. Šimánek, O. Černý, and R. Doleček: “EMC of Frequency Controlled Electric Drives”, Radioengineering, pp. 101-106, vol. 17, no. 4, Dec. 2008.
13. T. K. Sakar and A. Taaghoul: “Near-field to near/far-field transformation for arbitrary near-field geometry utilizing an equivalent electric current and MoM”, IEEE Transaction on Antennas and Propagation, vol. 47, pp. 566-573, Mar. 1999.
14. A. Taaghoul and T. K. Sakar: “Near-field to near/far-field geometry, utilizing an equivalent magnetic current”, IEEE Transnsaction Electro. Compatibility, vol. 38, pp. 536-542, Aug. 1996.
15. R. Laroussi and G. I. Costache: “Far-field predictions from near-field measurements using an exact integral equation solution”, IEEE Transnsaction Electromagnetic Compatibility, vol. 36, no. 3, pp. 189-195, Aug. 1994.
16. A. D. Yaghjian: “An Overview of Near-Field Antenna Measurements”, IEEE Transaction on Antennas and Propagation, vol. AP-34, no.1, Jan. 1986.